06 Oct 1971

Phase Velocities and Angle of Inclination for Frequency Components in Fully Developed Turbulent Flow Through Pipes

T. Hedrick

R. S. Azad

S. Banerjee

PHASE VELOCITIES AND ANGLE OF INCLINATION FOR FREQUENCY COMPONENTS IN FULLY DEVELOPED TURBULENT FLOW THROUGH PIPES*

T. Heidrick†
Atomic Energy of Canada Limited
Pinawa, Manitoba

R. S. Azad
University of Manitoba
Winnipeg, Manitoba

S. Banerjee††
Atomic Energy of Canada Limited
Pinawa, Manitoba

ABSTRACT

Measurements of phase shift and coherence between the streamwise velocity fluctuations at two sensors placed very close to each other have been made in fully developed turbulent flow in a smooth pipe. For the frequencies where the $\sqrt{\text{coherence}}$ is near unity (i.e. the correlation between the frequency components is near unity) the phase shifts have been related to the phase velocities and angle of inclination of a "frozen" pattern of turbulence.

Several other quantities such as intensities, energy spectral densities and mean velocities have also been obtained from the data taken with each sensor and these are in good agreement with previously found values. Probability densities of the streamwise velocity fluctuations were calculated and appear to be positively skewed near the wall and negatively skewed in the central region of the flow.

The phase shift measurements indicate that the phase velocities of all but the lowest frequency components are near and somewhat below the local mean velocity in the central region of the pipe and that the disturbance fronts are perpendicular to the wall. Near the wall all the disturbances seem to be inclined - the lower frequencies making smaller angles with the wall than the higher frequencies. The angles of inclination of all disturbances increase with distance from the wall. The phase velocity appears higher than the local mean velocity in this region.

INTRODUCTION

Turbulence structure near the wall in boundary layers and conduits has been extensively investigated by Schubauer and Klebanoff,[1] Laufer,[2] Klebanoff[3] and Townsend.[4] The measurements of auto correlations and power spectra were followed by spatial and space-time correlations reported by Grant[5] and Favre et al.[6,7] The space-time correlation measurements made up to 1964 were reviewed thoroughly by Favre.[8] Since then space-time correlations between the wall pressure and the three velocity components have been published by Willmarth and Tu[9] and in narrow frequency bands for the homogeneous directions in pipe flow by Morrison and Kronauer.[10] Even with these data it is difficult to infer a model for the turbulence structure near the wall and the best qualitative physical picture is probably that obtained from the flow visualization studies of Kline et al.[11]

The central difficulty lies in interpreting these space-time correlations in shear flows because the different Fourier components of the velocity field appear to move past measuring points at different velocities (or "celerities" - Favre). This problem (and the applicability of Taylor's hypothesis to shear flows) has been discussed by Lin,[12] Lumley,[13] Fisher and Davies[14] and Sternberg.[15] As Sternberg points out, the problem of interpretation is made even more difficult because structures or "vortices" appear to be inclined to the surface and the angle of inclination is a function of the scale of the motions. (This can be deduced from the time shifts for maximum correlation between two probes separated only in the direction perpendicular to the wall). In addition, there is the action of the mean shear on these structures which may cause a "rotation" about some "centre" where their convection velocity is equal to the local mean velocity. This effect shows up in that the line of maximum correlation between two probes is inclined to the wall and slightly curved, with the concave side facing away from the wall.[6]

The object of this work was to determine local convection velocities for the frequency components and the angle at which the disturbances are inclined to the wall. We have also found the probability densities of the streamwise velocity fluctuations and the skewness and kurtosis of these densities as a function of distance from the wall. The effect of the mean shear on the turbulence structure can be qualitatively inferred from these.

Theoretical Basis for Experiments

Consider a field which is homogeneous in the x and z directions, i.e. in planes parallel to the wall, but of finite energy in the y direction. The cross correlation function between u at y_1 and u at y_2 for all x and z separations will then be between unlike quantities and will not be symmetrical. The energy cross spectral density, G_{12}, which is the Fourier transform of the cross correlation, $F\{R_{uu}(y_1,y_2)\}$, will consist of a real and an imaginary part. The correlation function can be split into a sum of symmetric and anti-symmetric parts R_S and R_A. The Fourier transforms of these parts (in the homogeneous variables, x, z and t) $Co = F\{R_S\}$ and $iQ = F\{R_A\}$ may be written as the cross spectrum:

$$Co + iQ = (Co^2 + Q^2)^{\frac{1}{2}} \exp[i\theta] \qquad (1)$$

where $\theta = \text{Tan}^{-1}[Q/Co]$ - a function of k_x, k_z and ω.

If E_1 and E_2 are the spectral densities of u at y_1 and y_2 then we may define the coherence between u at y_1 and y_2 as:

$$Coh(k_x,k_z,\omega) = (Co^2 + Q^2)/E_1E_2$$

which is the square of the correlation between the Fourier components of u in the planes y_1 and y_2, without regard to phase differences. Coherence will fall off with increasing wave number and frequency.

For the range of frequencies and wave number where $Coh \cong 1$, the phase angle θ may be interpreted as the phase shift between the two signals. If the phase shift between two points fixed in the y_1 and y_2 planes, separated by a distance d, is measured as a function of ω, then a phase velocity in the direction of the line joining the two points can be defined as:

$$c(\omega) = \frac{\omega d}{\theta(\omega)} \qquad (2)$$

provided the disturbance front is perpendicular to the d - direction.

This definition is essentially the same as Lumley's[13] and Stegen and Van Atta's[16]. Stegen and Van Atta used this technique to measure phase velocities in grid turbulence and gave reasons supporting the accuracy of Equation 2 as long as $\sqrt{Coh}$ was near unity. It should be noted that even

---

*Work carried out in Atomic Energy of Canada's Whiteshell Nuclear Research Establishment

†Ph.D. Candidate attached to AECL

††Adjunct Professor, University of Manitoba

for a "frozen" pattern convecting past the two measuring points (implied by $\sqrt{Coh}$ near unity) there will be a distribution of phase velocity associated with each wave number, so the frequency, ω, and phase shift will contain contributions from all wave numbers. θ will be an average weighted on the basis of the energy contained in each wave number, i.e. the lower wave numbers traveling faster and containing more energy will contribute more to θ than will higher wave numbers traveling slower and with less energy. No information regarding the distribution of phase speeds for a given frequency or wave number can be obtained by this technique but the average value obtained has a clear significance. For $\sqrt{Coh}$ substantially less than unity the significance of the phase velocity is less clear since the turbulence pattern is "non-frozen".

In this paper we require that the $\sqrt{Coh} > 0.6$, i.e. the correlation coefficients for each frequency component be > 0.6. This is, of course, much stronger than requiring that the space-time correlation (which contains all components) be > 0.6 at the optimum time delay. The limit 0.6 is to some extent arbitrary and was chosen because the variance in our estimate of θ became quite large when $\sqrt{Coh}$ decreased below this value* (also discussed by Stegen and Van Atta). We are, at present, trying to find the lower limit of $\sqrt{Coh}$ for which the turbulence pattern can be considered frozen by varying d and measuring $\theta(\omega)$, $Coh(\omega)$ and deducing $c(\omega)$ from Equation 2. When d is increased $Coh(\omega)$ is reduced and the practical lower limit is reached when $c(\omega)$ deviates significantly from its original value.

Phase Shifts for a General Case

Equation 2 is derived for disturbance fronts perpendicular to the direction of separation of the two measuring points. A more general case is shown in Figure 1 where the disturbances in a frozen pattern are aligned at an angle α to the wall and the two probes are separated by a distance D at an angle β to the wall. The phase shift, θ_{12}, (lead of probe 1 over probe 2) is then:

$$\theta_{12} = \frac{\omega D}{c_x} (\sin \beta \cot \alpha - \cos \beta) \qquad (3)$$

In our experiments we are using probes of the configurations shown in Figure 2. From any two of these measurements c_x and α may be derived since:

when $\beta = 0$

$$\theta_{12} = \frac{D}{c_x},$$

when $\beta = \pi/4$

$$\theta_{12} = \frac{\omega D}{\sqrt{2}\, c_x} (\cot \alpha - 1), \text{ so if } \theta_{12} = 0, \alpha = \pi/4 \qquad (4)$$

If θ_{12} is positive, $\alpha < \pi/4$ without regard to the value of c_x if positive.

when $\beta = \pi/2$

$$\theta_{12} = \frac{\omega D \cot \alpha}{c_x}, \text{ so if } \theta_{12} = 0, \alpha = \pi/2 \qquad (5)$$

The data on phase shift we present in this paper are mainly for a probe of configuration I in Figure 2. We have processed some data for a probe of configuration II but have none from configuration III.

*The variance of the estimate is a function of the magnitude of the coherence and the statistical degrees of freedom, which depend on the bandwidth and sample size.

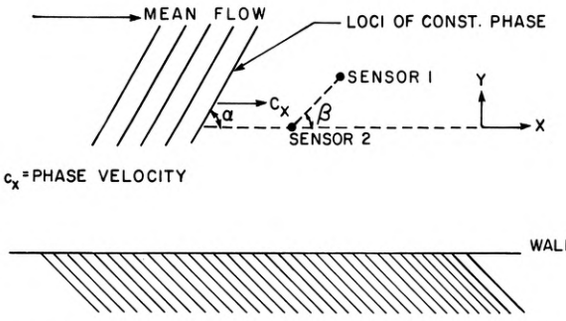

Figure 1: Schematic Diagram of Disturbance in a "Frozen" Pattern in Relation to Sensors and Wall

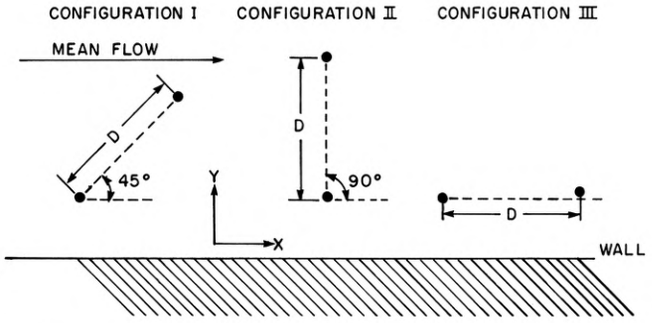

Figure 2: Configurations of the Two Sensor Probes Being Used in the Studies

EXPERIMENTAL

The turbulence measurements were made in water flowing through a straight smooth tube 24 ft. long and 3.1 in. I.D. The two anemometer signals were suitably processed and recorded on analog magnetic tape. The magnetic tape was then played to A-D converters which simultaneously converted the two channels into a digital tape. This could be used on AECL's CDC 6600 computer. The data were then processed using the fast Fourier transform algorithm of Cooley and Tukey.[17] The program also calculated intensities, correlation functions, probability density of the velocity fluctuations with skewness and kurtosis, coherence functions and phase shifts, frequency response functions and several other quantities.

The temperature of the flow system was controlled to 0.1°C. The data acquisition and processing equipment were checked for noise and electronic phase shifts and possible sources of error were eliminated.

RESULTS

A. Mean velocity, intensities and energy spectra

Every set of data was processed digitally for intensities, mean velocity and energy spectral densities. The intensities and mean velocities are shown in Figures 3, 4 and 5. The agreement with Laufer[2] and Burchill[18] is fairly good. From these and the energy spectral densities it was concluded that the two wires did not interfere. Typical energy spectral densities are shown in Figure 6 at various Reynolds numbers for $y^+ = 26$. The spectra for the two wires agree, are smooth and in excellent agreement with analog measurements. This is true for all the measurements. The loop and electronics appeared to be relatively free of noise.

B. Probability densities of the velocity fluctuations

Some probability densities at various y^+ and y/R for Reynolds number = 25,000 and 100,000 are shown in Figures 7 and 8 together with normal distributions with the same means and variances. The shape of these probability densities can be described in part by skewness and kurtosis and these are shown in Figure 9. The few results reported by Burchill are in fair agreement with ours. We believe the peaks and valleys in these curves are real, partially because they occur consistently in both the skewness and kurtosis, but we have no explanation for them yet.

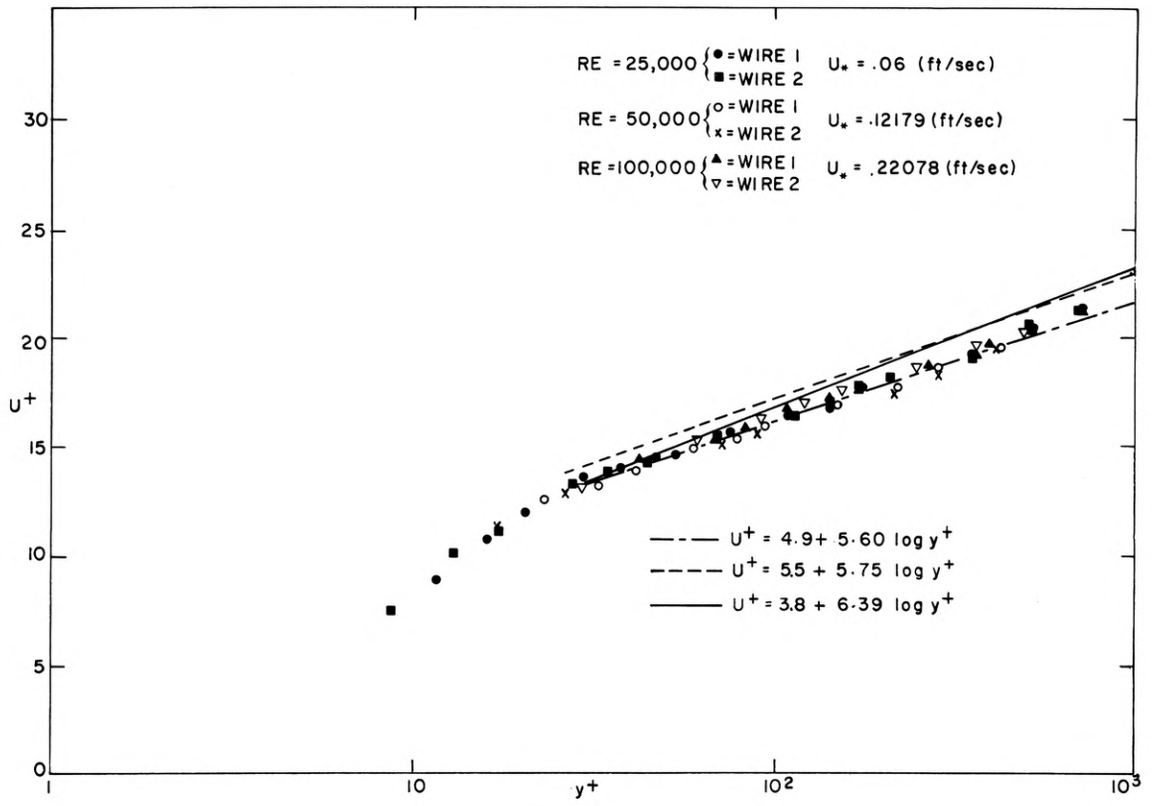

Figure 3: Mean Velocity Profiles Taken with Two Sensor Probes

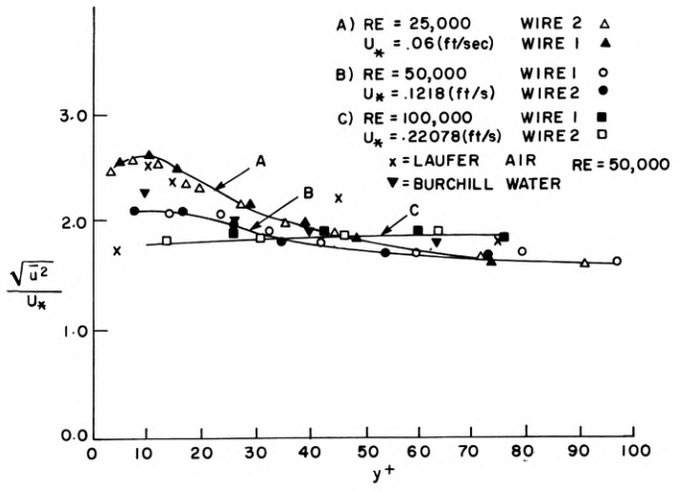

Figure 4: Turbulent Intensities in the Wall Region

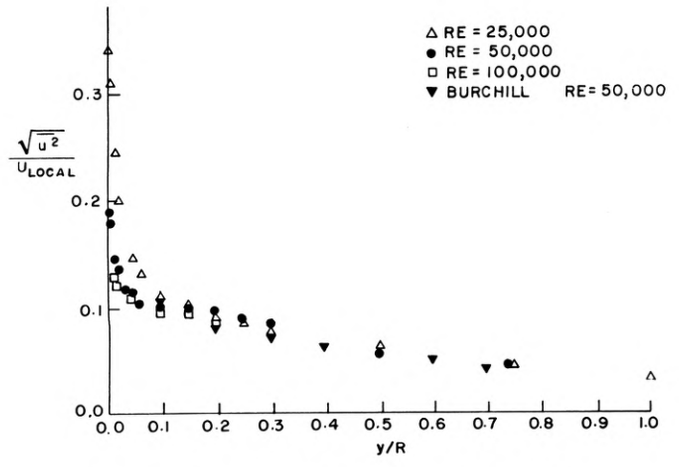

Figure 5: Turbulent Intensities in the Central Region

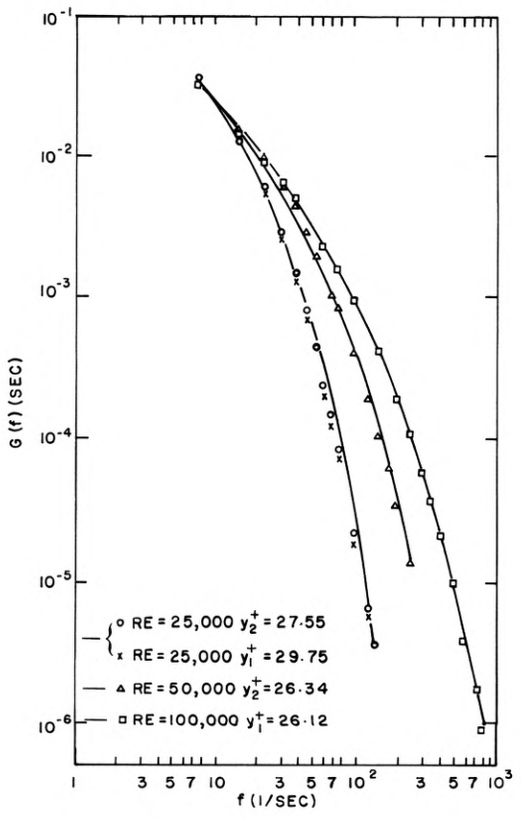

Figure 6: Typical Energy Spectral Densities

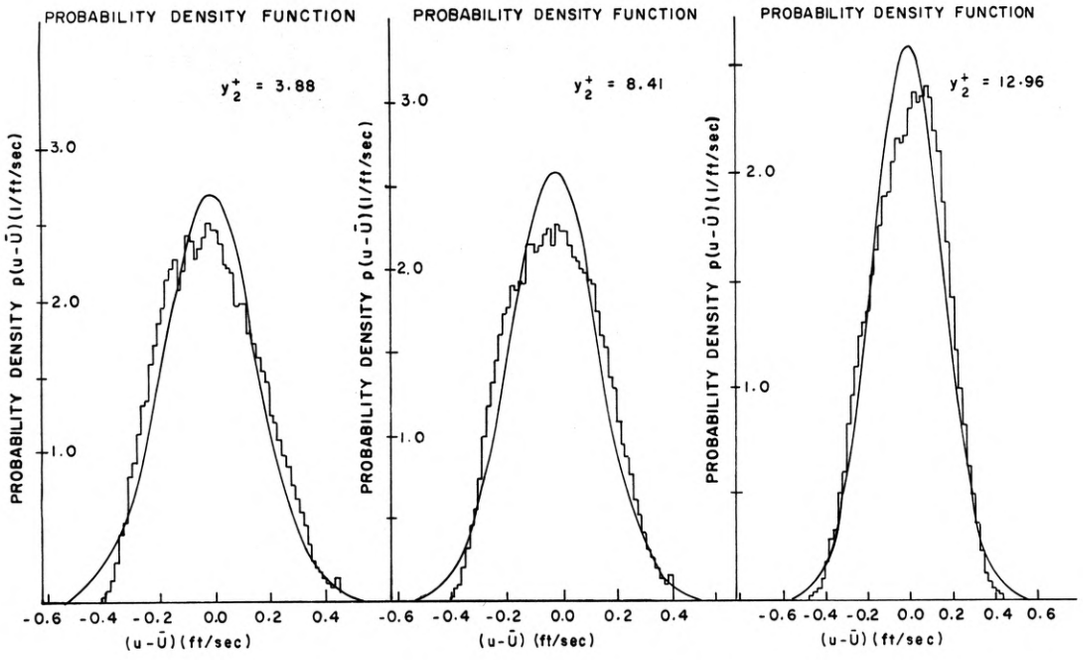

Figure 7: Probability Densities for the u-Fluctuations (at a Reynolds Number of 25,000)

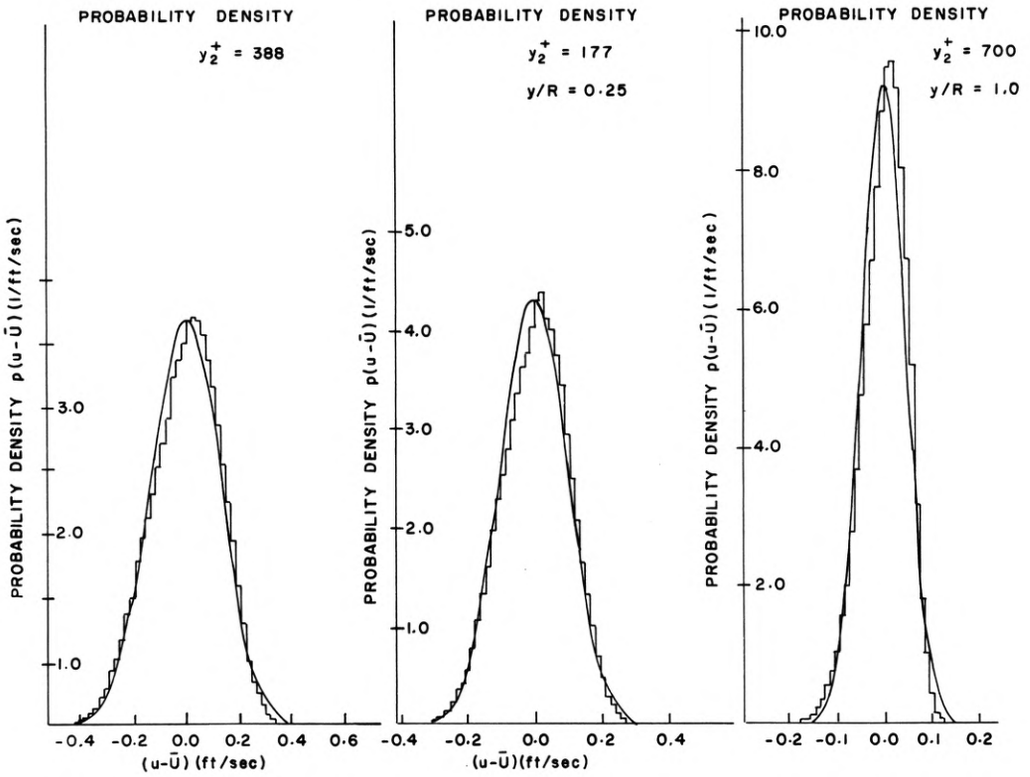

FIGURE 7 CONTINUED

The probability densities are positively skewed near the wall and negatively skewed toward the center. It is shown later that the phase velocities generally appear to be higher than the local mean velocity near the wall and lower or equal near the center. It follows that the positive skewing of the probability density is associated with phase velocities greater than the local mean velocity and vice versa. Fisher and Davies found a similar phenomenon in the mixing region of subsonic jets. The skewing is due to large negative or positive velocity fluctuations which are relatively infrequent and have a short time scale. This suggests that there are large scale motions which extend from the wall to the central region and are convected at some intermediate velocity. Their short time scales may be explained qualitatively by the rotating and stretching effect of the mean shear.

C. Phase shifts and phase velocities

The phase shifts measured with a probe of configuration I are shown in Figures 10, 11, 12, 13, 14 and 15. The dotted lines represent the phase shift to be expected if $\alpha = \pi/2$ (see Figure 1) and traveling at the local mean velocity. We have *also measured phase* shifts with a probe of configuration II but the results are only partially analyzed. These data were taken in the central region of the pipe at a Reynolds number = 100,000 and are given in Figure 16. The phase shifts for nearly all the frequencies do not appear to be significantly different from zero indicating that the disturbances are aligned perpendicular to the wall ($\alpha = \pi/2$) for $y/R > 0.3$.

The explanation for the data which we favor at present (but may modify as more results become available) is:

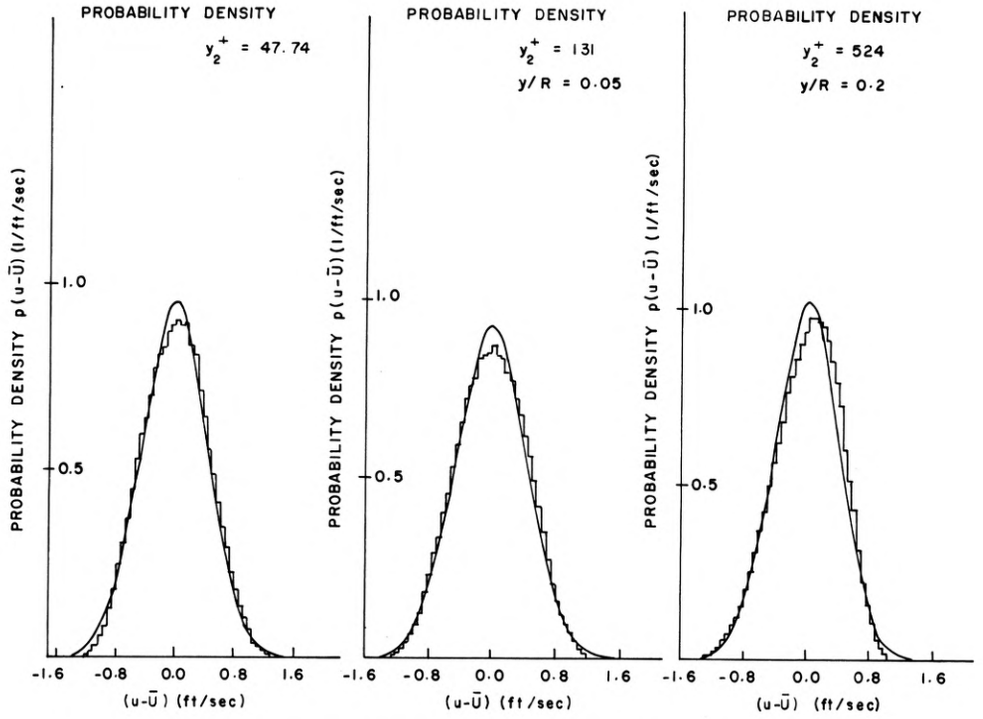

Figure 8: Skewness and Kurtosis of the Probability Densities Compared with Burchill's

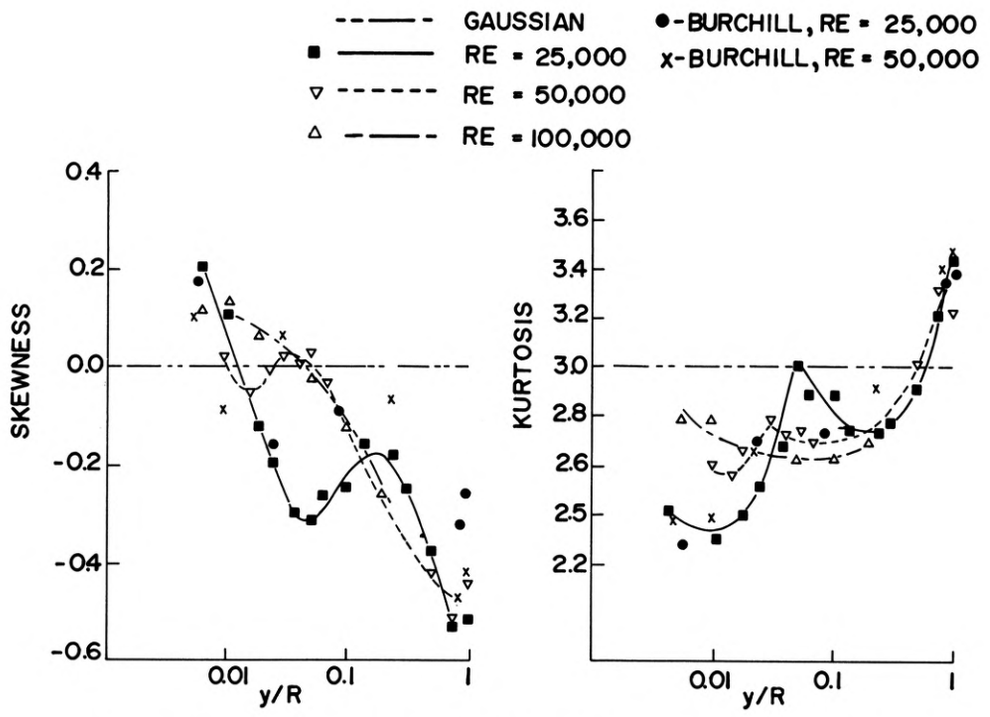

Figure 9: Skewness and Kurtosis of the Probability Densities Compared with Burchill's

(i) Disturbances in the central region of the pipe travel downstream at velocities quite close but somewhat below the local mean velocity. All but the very lowest frequencies have their fronts perpendicular to the wall.

(ii) The disturbances near the surface are inclined - the higher frequencies being less inclined than the lower frequencies. This is clear from the first two graphs in Figure 10. A positive phase shift, as pointed out after Equation 4 means that $\alpha < \pi/4$. So, qualitatively, the highest frequency disturbances are aligned at angles $> \pi/4$ very near the wall ($y^+ \sim 10$) but the lower frequency disturbances are inclined at $< \pi/4$. As we move away from the wall all the frequencies become progressively less inclined until at a $y^+ \sim 30$ they are inclined to the wall at 45^o.

(iii) At $y^+ \sim 150$ the phase shifts appear to be quite close to the phase shift if $\alpha = \pi/2$ and c_x is equal to the local mean velocity. Probably, α is close to $\pi/2$ for all the frequencies at this distance from the wall but we require to take more data with the probe of configuration II before drawing definite conclusions, i.e. the effect of α and c_x has to be separated by taking measurements with at least two known values of β.

(iv) If it is accepted for the present that $\alpha \sim \pi/2$ for all but the lowest frequencies at $y^+ \sim 150$ then the phase shifts suggest that $c_x >$ local mean velocity at distances that are closer to the wall and $c_x \lesssim$ local mean velocity at distances that are greater.

(v) For the central region the phase shifts appear to go through a

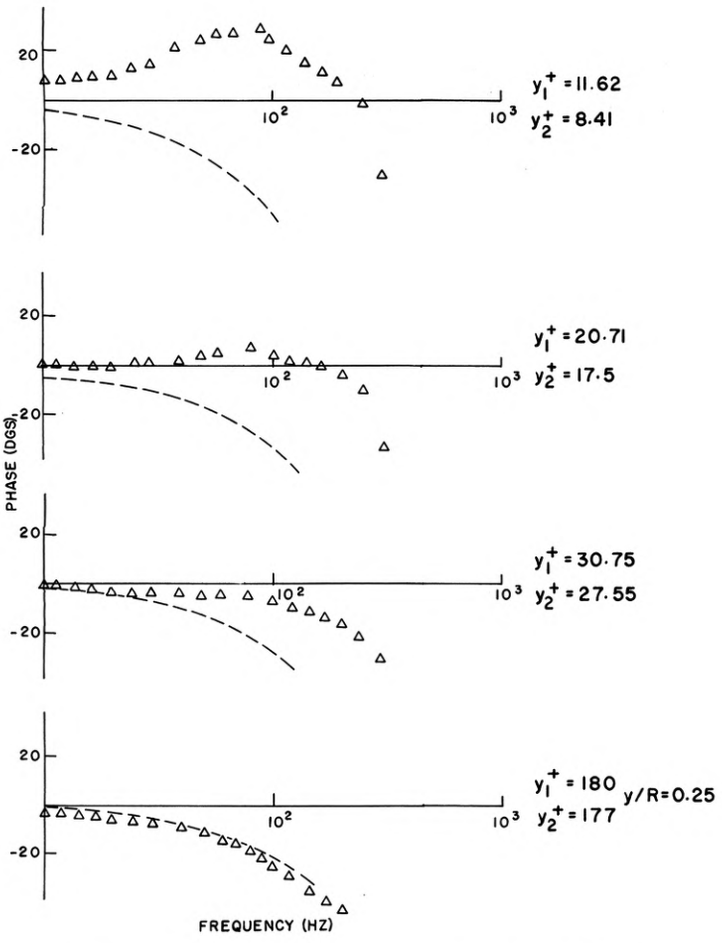

Figure 10: Phase Shifts for Re = 25,000 (Probe Configuration 1)

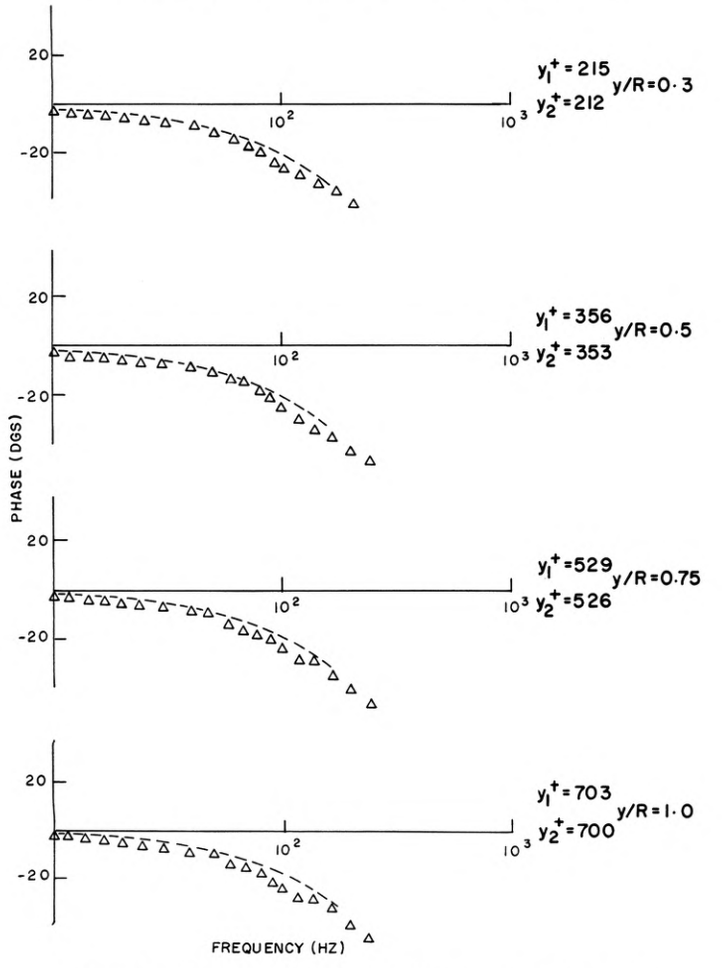

Figure 11: Phase Shifts for Re = 25,000 (Probe Configuration 1)

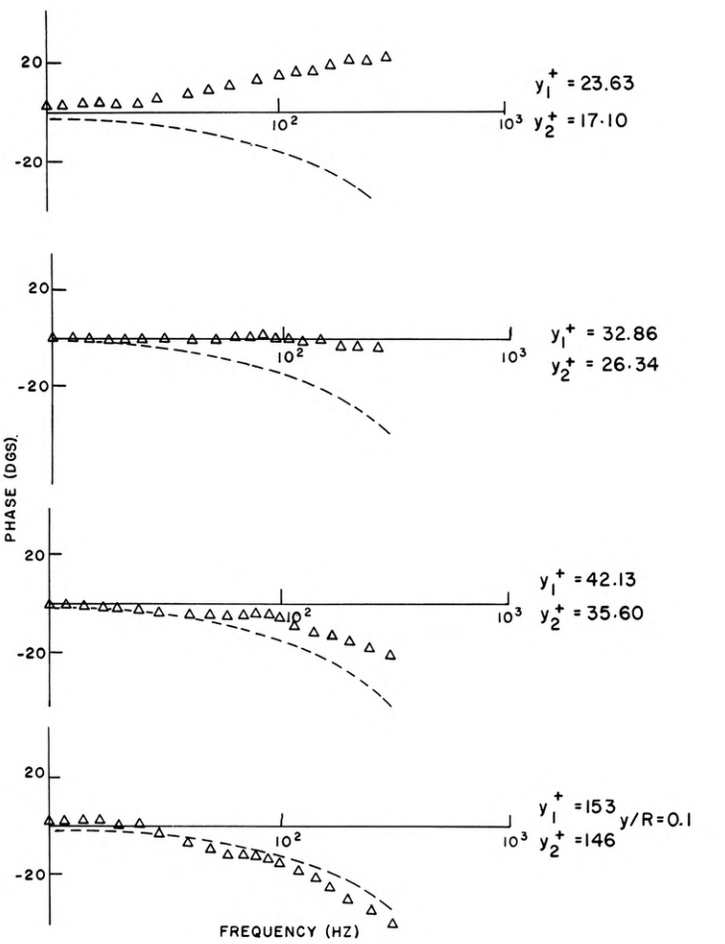

Figure 12: Phase Shifts for Re = 50,000 (Probe Configuration 1)

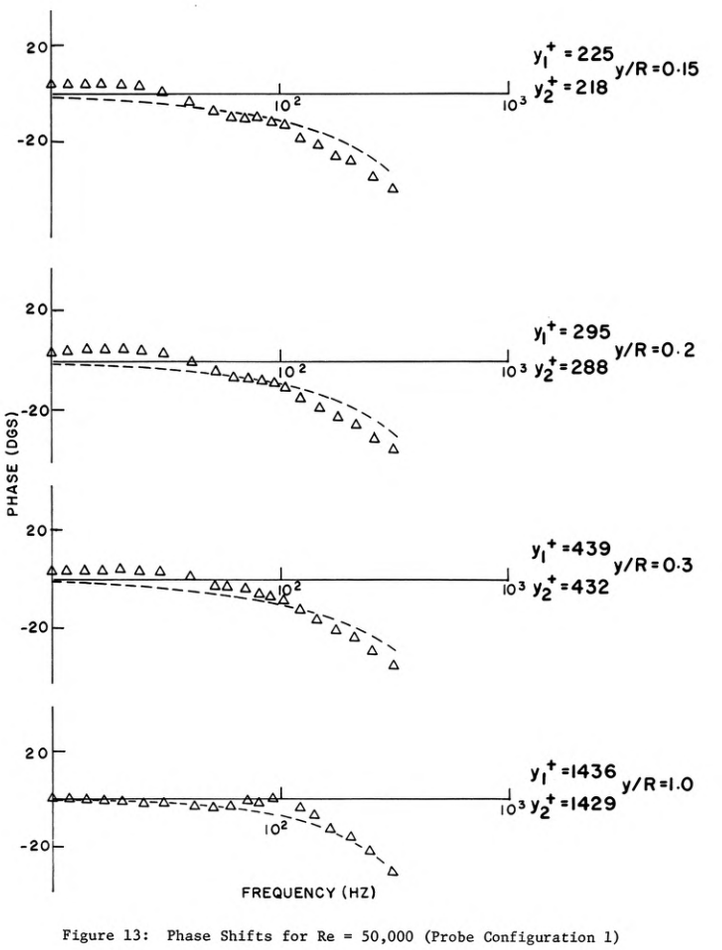

Figure 13: Phase Shifts for Re = 50,000 (Probe Configuration 1)

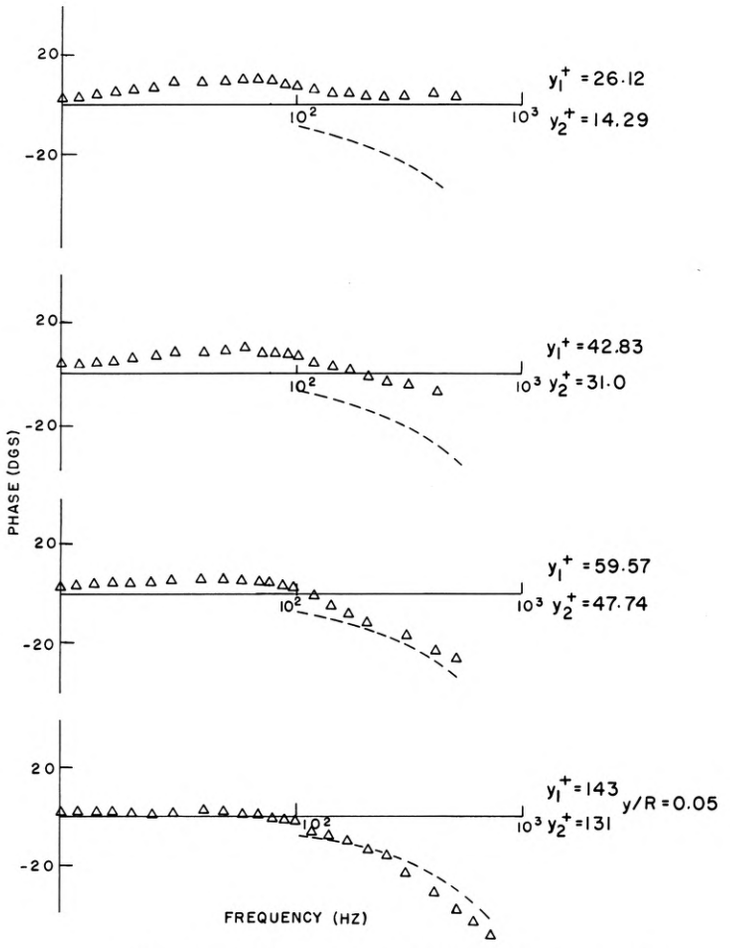

Figure 14: Phase Shifts for Re = 100,000 (Probe Configuration 1)

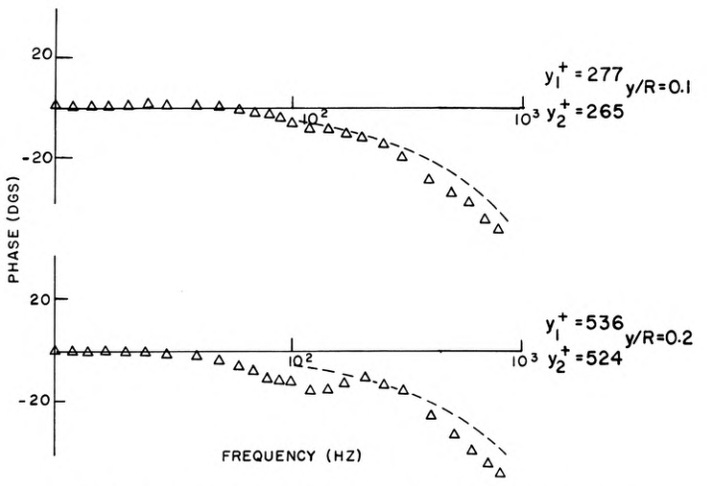

Figure 15: Phase Shifts for Re = 100,000 (Probe Configuration 1)

slight hump in a frequency range roughly midway between the highest and lowest frequencies shown. This is particularly pronounced for the higher Reynolds numbers, e.g. the last graph in Figure 15 (Re = 100,000). The phase shifts in the hump usually coincide quite closely with the dotted lines which represent the local mean velocity. These humps appear to be real and not due to aliasing, since we have sampled above the Nyquist frequency.

D. Coherences

The coherences for Reynolds numbers of 25,000, 50,000 and 100,000 are presented in Figures 17, 18 and 19 as a function of distance from the wall. There is a dip in the coherences in the mid-frequency range for the more central runs of the traverses at Reynolds numbers of 50,000 and 100,000. This dip becomes more pronounced as the center of the pipe is approached. Whether

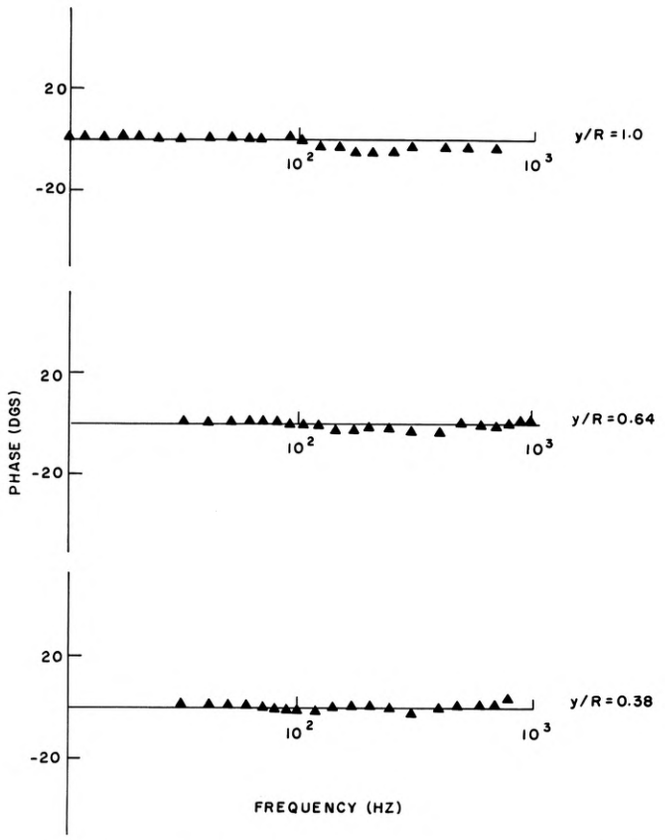

Figure 16: Phase Shifts for Re = 100,000 (Probe Configuration II)

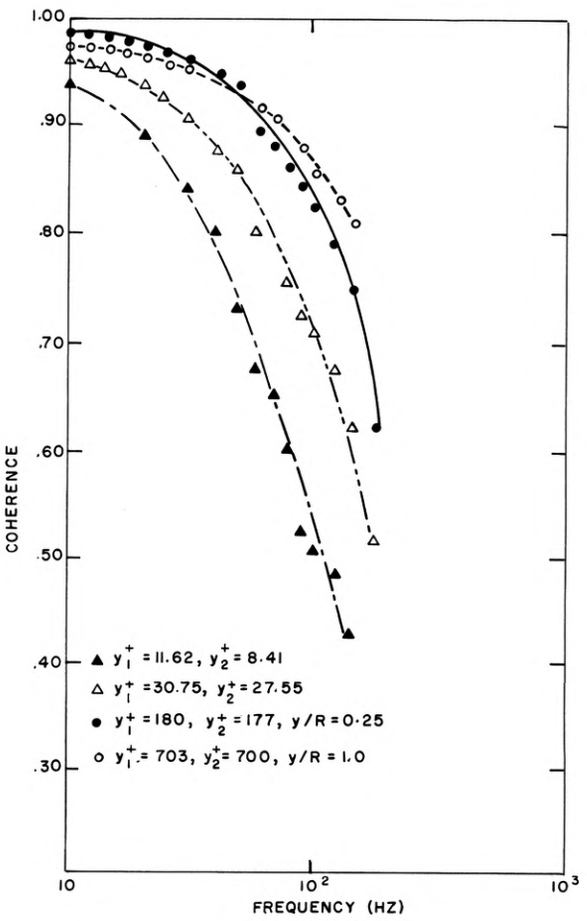

Figure 17: Coherences for Re = 25,000

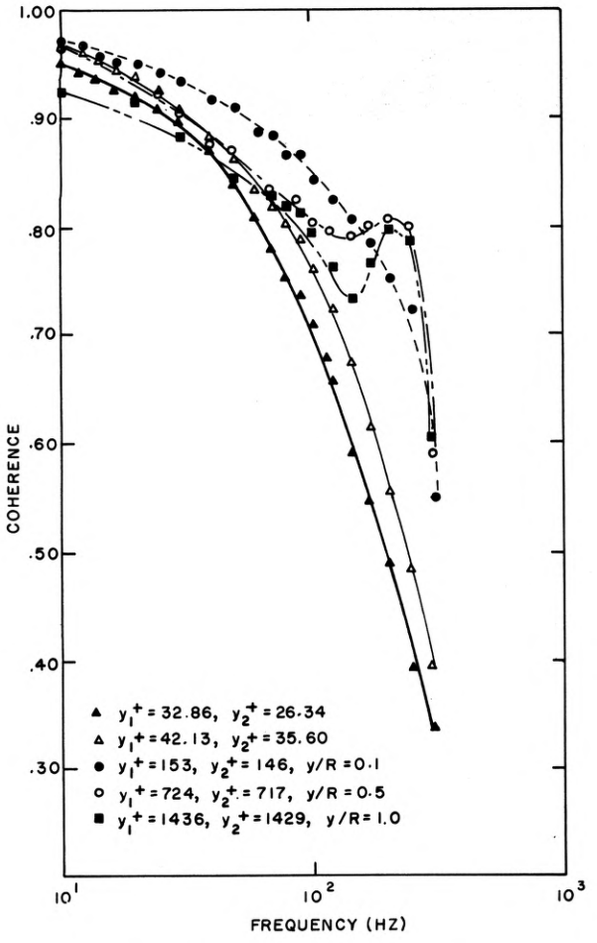

Figure 18: Coherences for Re = 50,000

this effect is fluid mechanic or electronic in origin is not yet known. Noise centered at this frequency would produce a loss in coherence which would become more pronounced as the signal level dropped due to lower turbulence levels. A program is presently underway to determine the cause of this effect.

SUMMARY

We have compared intensities, mean velocity profiles and energy spectra with published values for turbulent flow in pipes. The data appear to be good and there are no interferences between the two wires in our probes.

Probability distributions for the u fluctuations have been found together with their skewness and kurtosis. These indicate that large eddies extending from the central region of the pipe to the wall region may exist.

Phase shift and coherence measurements with probes of two geometries have been reported. This work is being continued, so results for Reynolds number = 25,000, 50,000 and 100,000 may be expected for all three probe geometries.

The phase shift measurements indicate that disturbances in the wall region are inclined. The lower frequencies are more inclined than the higher frequencies and the angles of inclination decrease with distance from the wall. At y^+ ~ 30 most of the disturbances (except the highest frequencies) are aligned at 45° to the wall. At a distance where y^+ ~ 150 most of the disturbance fronts are probably perpendicular to the wall and traveling at about the local mean velocity.

In the central region, the disturbances travel somewhat slower than the local mean velocity, whereas it appears likely that they travel somewhat faster for $y^+ < 150$.

There are dips in the coherence for some of the tests and a program is underway to determine their cause.

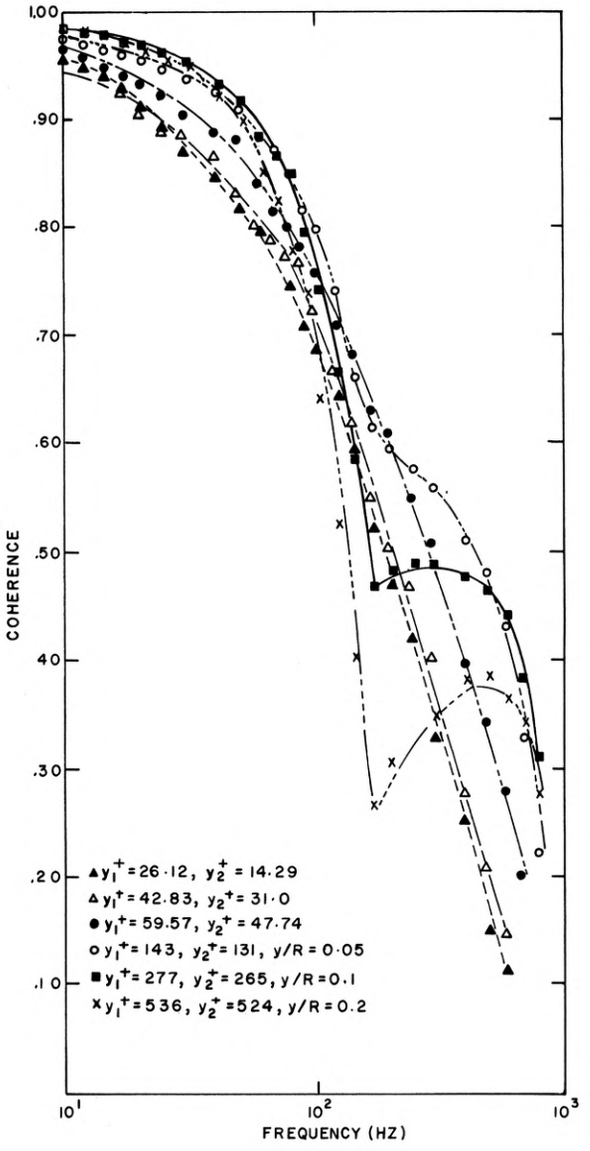

Figure 19: Coherences for Re = 100,000

The work is continuing and it is hoped that we will soon be able to present more quantitative data on angle of inclination and phase velocity for disturbances in the wall region.

SYMBOLS

c	phase velocity defined by Eq. 2
Co	Co-spectrum of u fluctuations at points 1 and 2, equal to the real part of G_{12}
Coh	coherence between u at points 1 and 2, equal to the magnitude squared of G_{12}, divided by the product of E_1 and E_2
c_x	phase velocity in the axial direction
d,D	probe separation
f	frequency (Hz)
G_1, G_2, E_1, E_2	normalized one dimensional energy spectral density of the u fluctions at points 1 and 2 respectively
G_{12}	cross spectral density of u fluctuations at points 1 and 2 (in general complex)
k_i	wave number component in the i'th direction
Q	Quadrature spectrum of u fluctuations at points 1 and 2, equal to the imaginary part of G_{12}
RE	Reynold's number based on bulk average velocity
R	pipe radius
$R_{uu}(y_1,y_2)$	correlation coefficient between u at y_1 and y_2, a function of $x_1 - x_2$, $z_1 - z_2$ and time delay

$\overline{U}$	local mean velocity
u	axial component of the fluctuating velocity
u^+	dimensionless velocity (u/u_*)
u_*	friction velocity
y_1^+, y_2^+	dimensionless distance from the wall of wire 1 and 2 respectively (yu_*/ν)
α	angle between loci of constant phase and axial direction (as shown, Figure 1)
β	angle between line joining sensors and axial direction (as shown, Figure 1)
θ_{12}	phase angle of the complex spectrum, G_{12}, defined in Equation 1
ω	angular frequency ($2\pi f$)
ν	kinematic viscosity

REFERENCES

1. Schubauer, G. B. and Klebanoff, P. S., NACA Report 1030 (1951).
2. Laufer, J., NACA TN 2954 (1953).
3. Klebanoff, P. S., NACA TN 3178 (1954).
4. Townsend, A. A., "The Structure of Turbulent Shear Flow", Cambridge University Press, London, 1956.
5. Grant, H. L., J. Fluid Mech., 4, 149 (1958).
6. Favre, A. J., Gaviglio, J. J., and Dumas, R., J. Fluid Mech., 2, 313 (1957).
7. Favre, A. J., Gaviglio, J. J., and Dumas, R., J. Fluid Mech., 3, 149 (1958).
8. Favre, A. J., J. Appl. Mech., 22, 241 (1965).
9. Willmarth, W. W. and Tu, B. J., Physics of Fluid Supplement, S134 (1967).
10. Morrison, W. R. B. and Kronauer, R. E., J. Fluid Mech., 39, 117 (1969).
11. Rundstadler, P. W., Kline, S. J. and Reynolds, W. C., Stanford University Report MD-8, (1963).
12. Lin, C. C., Quart. Appl. Math., 10, 295 (1953).
13. Lumley, J. L., Phys. Fluids, 8, 1056 (1965).
14. Fisher, M. J. and Davies, P. O. A. L., J. Fluid Mech., 18, 97 (1964).
15. Sternberg, J., Physics of Fluid Supplement, S146 (1967).
16. Stegen, G. R. and Van Atta, C. W., J. Fluid Mech., 42, 689 (1970).
17. Cooley, J. W. and Tukey, J. W., Math. of Comput., 19, 297 (1965).
18. Burchill, W. E., "Statistical Properties of Velocity and Temperature in Isothermal and Nonisothermal Turbulent Pipe Flow", Ph.D. Thesis, University of Illinois, 1970.